

RSC Advances



This is an *Accepted Manuscript*, which has been through the Royal Society of Chemistry peer review process and has been accepted for publication.

Accepted Manuscripts are published online shortly after acceptance, before technical editing, formatting and proof reading. Using this free service, authors can make their results available to the community, in citable form, before we publish the edited article. This *Accepted Manuscript* will be replaced by the edited, formatted and paginated article as soon as this is available.

You can find more information about *Accepted Manuscripts* in the [Information for Authors](#).

Please note that technical editing may introduce minor changes to the text and/or graphics, which may alter content. The journal's standard [Terms & Conditions](#) and the [Ethical guidelines](#) still apply. In no event shall the Royal Society of Chemistry be held responsible for any errors or omissions in this *Accepted Manuscript* or any consequences arising from the use of any information it contains.

Effects of Acid-alkaline Environment on the Reactivity of the 5-Carboxycytosine with Hydroxyl Radical

Lingxia Jin^{*a} Caibin Zhao^a Tianlei Zhang^a Zhiyin Wang^a Suotian Min^a
Wenliang Wang^{*b} Yawen Wei^c

^a*Shaanxi Province Key Laboratory of Catalytic Fundamentals & Applications, School of Chemical & Environment Science, Shaanxi University of Technology, Hanzhong, Shaanxi 723001*

^b*Key Laboratory for Macromolecular Science of Shaanxi Province, School of Chemistry and Chemical Engineering, Shaanxi Normal University, Xi'an 710062*

^c*Institute of publication Science, Chang'an University, Xi'an 710064*

ABSTRACT

Hydroxyl radical ($\bullet\text{OH}$) is produced in biological systems by external or endogenous agents. It can damage DNA/RNA by attacking pyrimidine nucleobases through the addition reaction and H-atom abstraction. However, the correlation study for the new cytosine derived DNA modification (5-Carboxycytosine, 5-caCyt) remains scarcely existent. Here three distinct groups of mechanisms for 5-caCyt with $\bullet\text{OH}$ at the CBS-QB3 approach have firstly been explored, the direct reaction (paths R1~R6), acid (paths R1'~R3', R5', R6'), and alkaline (paths R1''~R5'')-induced processes, respectively, and it indicates that the addition of $\bullet\text{OH}$ to the C5=C6 double bond of 5-caCyt is more favourable in neutral, acid and alkaline conditions, and the ΔG^{\ddagger} value of C5 channel is a little higher than that of C6 route, which agrees with the tendencies observed

* Corresponding authors. Tel: +86-916-2641660; e-mail: jinxl@snut.edu.cn (L.X. Jin); Tel: +86-29-81530815 Fax: +86-29-81530727; e-mail: wjwang@snnu.edu.cn (W. L. Wang).

†Electronic supplementary information (ESI) available: The relevant energy information on different protonated 5-caCyt isomers both in the gas and aqueous phases is listed in Tables S1. The comparison of the activation free energies by G3B3 and CB3-QB3 composite approaches are listed in Table S2. Spin contamination ($\langle S^2 \rangle$) and after spin annihilation ($\langle S_a^2 \rangle$) values in $\bullet\text{OH}$ -mediated 5-caCyt, 5-caCytN3⁺ and 5-CytCOO⁻ reactions are listed in Tables S3. The relevant energy information on different 5-caCyt isomers both in the gas and aqueous phases is listed in Tables S4. The relative energies for the addition of $\bullet\text{OH}$ to C2, N3, C4, C7 sites of 5-caCyt both in the gas and aqueous phases are listed in Tables S5. The nucleus-independent chemical shifts (NICS(0)) for the product radicals of $\bullet\text{OH}$ abstraction from 5-caCyt in the gas phase are given in Table S6. The relative energies for the addition of $\bullet\text{OH}$ to C2, C4, C7 sites and the H4 atom abstraction of 5-caCytN3⁺ both in the gas and aqueous phases are listed in Table S7. The NPA charge on O of $\bullet\text{OH}$ for path R4 in the gas (a) and aqueous phases (b) are listed in Table S8. The corresponding geometrical structures of protonated 5-caCyt and 5-caCyt isomers in the aqueous phase are listed Figs.S1 and S2. The potential energy surface (ΔG^{\ddagger} in kJ·mol⁻¹) along the addition of $\bullet\text{OH}$ to C2, N3, C4, C7 sites of 5-caCyt in the gas phase is listed Fig.S3. The potential energy surface (ΔG^{\ddagger} in kJ·mol⁻¹) along the addition of $\bullet\text{OH}$ to C2, C4, C7 sites and the abstraction H4 atom of 5-caCytN3⁺ in the gas phase is listed Fig.S4. The important bond lengths of all stationary points for the main addition and hydrogen abstraction paths in neutral, acid and alkaline conditions in the aqueous phase are listed in Figs.S5~S13.

experimentally. Moreover, the H5 abstraction in alkaline media might be competitive with the addition reactions, having a ΔG^{\ddagger} value of 32.55 kJ·mol⁻¹, which is only 17-20 kJ·mol⁻¹ more energetic than for the addition reactions. In addition, the ΔG^{\ddagger} values of the •OH reactions are slightly lower for the neutral or deprotonated systems than for the N3-protonated 5-caCyt, implying that the reaction trends are a little enhanced. Our results give a possible new insight on the 5-caCyt in the presence of •OH for the experimental scientists.

1. Introduction

The hydroxyl radical (•OH) is an important ROS, which is usually present at very low levels in biological systems, mainly arising from oxygen metabolism. Its concentration is markedly enhanced upon exposure of cells to exogenous chemical and physical agents, such as ionizing radiation. Cells have mechanisms to palliate the toxicity of •OH when its concentration is low.^{1,2} However, at higher concentrations, the damage is unavoidable and the development of age-dependent diseases such as cancer, arteriosclerosis, arthritis, neurodegenerative disorders are prevailing.^{3,4}

The recently discovered nucleobase 5-carboxylcytosine (5-caCyt) is the final product of oxidative attack on the C5 position of cytosine (Cyt) by TET proteins,⁵⁻⁸ which has been proposed as the eighth DNA base. It can be removed from DNA and replaced by Cyt via base excision repair.⁹ A study recently demonstrated that 5-caCyt in mouse embryonic stem cells may recruit unique proteins for certain functions; It could be more than the intermediates in the DNA demethylation pathway.¹⁰ Moreover, the experiments recently demonstrated that 5-caCyt can change the fidelity of DNA replication and slow down RNA polymerase II transcription, suggesting the possible functional roles of 5-caCyt occur on DNA replication and transcription.^{11,12} On the contrary, it is still unclear whether 5-caCyt plays functional roles in cancer development and formation.¹³ According to the literature,¹⁴ the development of certain cancers is interconnected with oxidative damage by hydroxyl radical. It can oxidize the DNA bases either by addition or hydrogen abstraction reactions to produce damaged bases or strand breaks.^{15,16} For instance, Zuo et al.¹⁷ discovered that OH radical preferentially added to C5 and C6 sites of 5-MeCyt would produce the pyrimidine glycol, leading to the deamination of 5-MeCyt to thymine. Von Sonntag et al.¹⁸ demonstrated that the hydrogen abstraction from the methyl group, which gave rise to the methyl radical of the pyrimidine bases. Those radicals may react with the neighboring nucleobases to cause the damage of cell function. Therefore, the reactions of •OH with 5-caCyt are also likely to happen and might also lead to the damaged DNA bases to cause the formation of cancer. Moreover, the early experiments¹⁹ have reported that the adduct radicals are mainly formed by addition of •OH to C5 and C6 sites of 5-caCyt in solution. As for 5-caCyt, it still possesses three double bonds and five H atoms, respectively, and what is to become of them in the face of •OH?

It has been demonstrated in experiments that there are three prevailing species of the 5-caCyt moiety in 5-carboxyl-2'-deoxycytidine (R=2'-deoxyribose) at different pH, the cationic and

anionic 5-caCyt, and the zwitterionic 5-caCyt[±] species, respectively.²⁰ Portalone et al.²¹ have reported that only the anionic (b) and zwitterionic forms (c) have been detected in solution in the pH range 2.0-9.0 (Fig. 1). Unfortunately, the zwitterionic 5-caCyt[±] form is failed to be optimized due to amino-imino conversion by means of theoretically calculation.²¹⁻²³ The anionic form (5-CytCOO⁻) in the experimental studies has been artificially introduced in double-stranded DNA, and on the contrary the cationic form is not expected in cellular DNA at physiological conditions.²⁰ The existence of the N3-protonated form (a) has been postulated at pH <1 (Fig. S1 and Table S1).^{20,21} However, this strongly acidic pH, the DNA macromolecule should be hydrolysed,²⁴ and the protonation of N3 site for 5-caCyt (5-caCytN3⁺) could not exist in the DNA in vivo. Therefore, the deprotonation of C5-carboxylic group (5-CytCOO⁻) and neutral 5-caCyt will be considered, raising that the question of whether there is competition between them treated with •OH. Meanwhile, for contrast, the •OH-mediated 5-caCytN3⁺ reactions have also been reported in this paper. Moreover, until now the experimental data of these reactions in solution are vanishingly rare.

As mentioned above, the •OH-mediated addition and H-atom abstraction mechanisms of the 5-caCyt and 5-CytCOO⁻ are firstly explored from a theoretical perspective to clarify whether the •OH-mediated processes of 5-caCyt can kinetically compete with their 5-CytCOO⁻. Meanwhile, the reaction mechanisms and activation free energies of 5-caCyt and 5-CytCOO⁻ have been performed a comparison with their 5-caCytN3⁺ in the presence of •OH. Our results give a possible new insight on the 5-caCytN3⁺ and 5-CytCOO⁻ under abnormal environments such as hypoxia or hyperoxia.

2. Computational methods

All the calculations were performed using the Gaussian 09 package.²⁵ The more reliable energies were conducted at the CBS-QB3 level of theory.²⁶ Specifically, the CBS-QB3 method involves the following steps: B3LYP/6-311G (2d,d,p) geometry optimization; B3LYP/6-311G (2d,d,p) frequency calculation with a 0.99 scale factor for the ZPE; CCSD (T)/6-31+G* energy calculation; MP4 (SDQ)/6-31+G(d(f),p) energy calculation; UMP2/6-311+G(3d2f,2df,2p) energy calculation and CBS extrapolation. In addition, this approach includes empirical corrections for spin contamination.

To test the reliability of CBS-QB3 method, single point computation was also done using G3B3 approach.²⁷ It is clear from Table S2 that the activation free energies calculated using both the different methods agree well with each other, proving that these two approaches are able to provide reliable data for our system.

Moreover, many previous investigations have proposed that the CBS-QB3 method can provides adequately accurate energies, with a standard deviation of about 1.5 kcal•mol⁻¹.²⁸⁻³⁰ The CBS-QB3 method also has been used to calculate ΔG values for deprotonation system where the experimental values are reported to be accurate within 1 kcal•mol⁻¹.³¹ We note that the CBS-QB3 methodology includes a correction for spin contamination in open-shell species.^{26,32-37} Therefore,

the CBS-QB3 method was selected for radical additions to unsaturated bonds because these kinds of transition states suffer from spin contamination.

All the stationary points including reactant complexes, transition states, and products have been optimized using CBSB7 (B3LYP/6-311G (2d,d,p)) method. Vibrational frequency calculations have been conducted at the level of theory used for optimization to characterize the nature of each stationary point as a minimum (real frequencies) or transition state (only one imaginary frequency) and to correct energies for zero-point at 298.15 K. Intrinsic reaction coordinate (IRC)³⁸ calculations have been carried out at the same level of theory from each transition state to ensure that the obtained transition states connected the appropriate reactants and products. Besides, the obtained stationary points based on the gas phase geometries have been further optimized using polarized continuum model (PCM)³⁹ at CBS-QB3 method, with dielectric constant 78.39 to simulate the aqueous environment. Additionally, the activation free energies in the gas (ΔG^{\ddagger}) and aqueous phases (ΔG^{\ddagger}) calculations have been obtained at 298.15 K.

Finally, the nucleus-independent chemical shifts (NICS(0)) in the centers of the six-membered heterocyclic compounds of the lowest energy structures for the product radical are determined by GIAO/DFT procedure (the gauge-independent atomic orbital/density functional theory).⁴⁰ The Natural Population Analysis (NPA) charges have been used to analyze the difference of the reaction trend in the gas and aqueous phases. They were calculated at the CBS-QB3 method,²⁶ adopting natural population analysis.^{41,42}

3. Results and discussion

The expectation values of $\langle S^2 \rangle$ for all species contained in these reaction systems are listed in Table S3. After spin annihilation, the values of $\langle S^2 \rangle$ for open-shell systems are very close to 0.7500, indicating that the spin contamination can be negligible at the above mentioned computation level.

In neutral condition, as for 5-caCyt, there are two isomers based on the torsion and angle of the COOH group, denoted as M1 and M2, respectively (Fig. S2 and Table S4), and M1 both in the gas and aqueous phases are more stable than M2. Thus on the basis of this result, the more stable M1 isomer has been chosen for the present computational study. As seen from Fig. S2, the dihedral angles are all 0.0° for the pyrimidine ring of 5-caCyt, suggesting a planar geometry and the ring π -system. The corresponding dihedral angles are also 0.0° for the exocyclic group of 5-caCyt, implying that the more planar character is found in C=O, -NH₂, and -COOH of 5-caCyt, respectively. The constituent atoms of these bonds are expected to be more reactive for the electrophilic addition reaction with hydroxyl radical. The structural features of 5-caCyt are favored C2, O2, N3, C4, C5, C6, C7, and O3 as the addition sites. As for the O2 and O3 sites, various initial geometries of adducts have been designed, but the •OH is always far from O2 and O3 atoms. As for the •OH addition to C2, N3, C4, C5, C6 and C7 sites of 5-caCyt (Tables 1 and S5, Fig. S3), the ΔE^{\ddagger} values between the initial reactants and the TSs are 58.51, 62.68, 45.11, 4.03, 1.07 and 63.10 kJ·mol⁻¹, respectively, suggesting that the •OH addition to C5 and C6 sites

are kinetically more favorable than to other sites. Moreover, the addition of $\bullet\text{OH}$ to C5 and C6 sites are highly exothermic with respect to their energies of the reaction complexes, whereas the reactions of other sites are endothermic relevant to their energies of the reaction intermediates. These results imply that the addition of $\bullet\text{OH}$ to the C5 and C6 sites for 5-caCyt are both thermodynamically and kinetically more favorable than addition to other sites, and have higher reaction probability. In contrast, the very lower probability is happen in the addition of C2, N3, C4 and C7 sites. The results are in agreement with the experimental result¹⁹, which showed no evidence for addition at C2, N3, C4 and C7 sites. The same conclusion exists in the aqueous phase. Therefore, only the addition of $\bullet\text{OH}$ to the C5=C6 bond for 5-caCyt has been investigated in this paper. Meanwhile, there are five abstractable hydrogen atoms viz. the H3 and H4 attached to N4, the H5 attached to C6, the H6 attached to O4, and the H7 attached to the N1. The H7 abstraction reaction here is neglected, and the reason is that N1 of the 5-caCyt is always bonded to a carbon of the deoxyribose in the real case of DNA.

3.1 Stationary point structures and energetics in the gas phase

Since $\bullet\text{OH}$ has extremely high chemical reactivity, the various complexes can be formed with 5-caCyt. The two cases in which the H and O of $\bullet\text{OH}$ are pointed toward the π -face of 5-caCyt have initially been considered, leading to the π -bonded and H-bonded complexes formed in these reactions (see Fig. 2). For the H-bonded complex, the H-bond is formed by the N or O of 5-caCyt and H of $\bullet\text{OH}$ as well as the H of 5-caCyt and the O of $\bullet\text{OH}$. As for a π -bonded complex, the π -bond is formed by the O of $\bullet\text{OH}$ with C of 5-caCyt. According to the literature,⁴³ the energy of the H-bond depends on the $\text{Y}\cdots\text{H}$ distance and the $\text{X-H}\cdots\text{Y}$ angle (where X is a hydrogen donor and Y is a hydrogen acceptor). According to the $\text{Y}\cdots\text{H}$ distances, all H-bonds can be divided into strong ($\text{Y}\cdots\text{H}<1.600$ Å), medium ($\text{Y}\cdots\text{H}=1.600$ - 1.900 Å), and weak ($\text{Y}\cdots\text{H}>1.900$ Å). According to the range of $\text{Y}\cdots\text{H}$ distances and the number of H-bond, the H-bond in complexes should be assigned as weak and medium (as shown in Fig 2).

In IM1, the distances for O of $\bullet\text{OH}$ with C5 and C6 are 2.427 and 2.511 Å, respectively, implying that it is a typical π -bonded complex. Similar with IM1, the distances for O of $\bullet\text{OH}$ with C5 and C6 in IM2 are 2.417 and 2.486 Å, respectively, which is also a typical π -bonded complex. Dissimilar with IM1 and IM2, in IM6, the H of $\bullet\text{OH}$ forms an H-bond with O3 of 5-caCyt at a distance of 1.897 Å, and the O of $\bullet\text{OH}$ also forms H-bond with H6 of 5-caCyt at a distance of 1.868 Å, which is a typical H-bonded complex. Identify with IM6, two hydrogen bonds in IM5 formed, the distances of $\text{C7-O4}\cdots\text{H1}$ and $\text{H5}\cdots\text{O1-H1}$ are 1.987 and 2.279Å, respectively. For IM3 and IM4, the H-bonded complex formation is mainly aroused from the interactions of the lone pairs on the N3 and O3 atoms with the hydrogen of $\bullet\text{OH}$, respectively. According to the relative energy values (ΔE^{e}), the order of stability for the reaction complex is $\text{IM6}\approx\text{IM3}>\text{IM4}>\text{IM2}>\text{IM5}\approx\text{IM1}$ (see in Table 1).

3.1.1 The reaction mechanism of OH-mediated 5-caCyt

Addition reaction mechanism. As mentioned above, the $\bullet\text{OH}$ can add to C5 and C6 sites of

5-caCyt denoted as R1 and R2, respectively. As seen in Figs. 2 and 3, in path R1, the $\bullet\text{OH}$ firstly forms a π -bonded complex IM1. With the approaching of $\bullet\text{OH}$, the $\text{O1}\cdots\text{C6}$ bond has been cleaved, and then adds to the C5 site *via* transition state TS1 with a ΔG^{\ddagger} value of only $2.64 \text{ kJ}\cdot\text{mol}^{-1}$, leading to the formation of P1 (Fig.4 and Table 1). In P1, the C5 atom has a tetrahedral structure, and the distances of C5–C4, C5–C6, and C5–C7 are stretched to 1.538, 1.477, and 1.536\AA , respectively, longer than those in IM1 (1.462 \AA for C5–C4, 1.386 \AA for C5–C6, and 1.461 \AA for C5–C7), suggesting that the hybridization of C5 atom converts from sp^2 in IM1 to sp^3 in P1 and the C5=C6 double bond turns into a single bond. Indentify with path R1, the IM2 is converted into P2 via transition state TS2 associated with a ΔG^{\ddagger} value of $8.12 \text{ kJ}\cdot\text{mol}^{-1}$. As seen from Table 1, the ΔE^{\ddagger} values of P1 and P2 are -51.39 and $-92.61 \text{ kJ}\cdot\text{mol}^{-1}$, respectively. The spin maxima values also come to the same conclusion that is the higher delocalization of the unpaired electron in P2 (Table 2 and Fig. 5). These indicate that $\bullet\text{OH}$ addition to C6 site would be thermodynamically more favorable than to C5 site. However, there is a little small energy barrier for the $\bullet\text{OH}$ addition to C6 site, while there is nearly barrierless ($2.64 \text{ kJ}\cdot\text{mol}^{-1}$) for addition to C5 site. This implies that the $\bullet\text{OH}$ addition to C5 site is a little more kinetically favorable than to C6 site, which agrees with $\bullet\text{OH}$ addition at C5 site preferentially in experiment.¹⁹

H-atom abstraction. In this section, the $\bullet\text{OH}$ is abstracting from the H3 and H4 of NH_2 group, the H5 of cyclic C6, and the H6 of COOH group for 5-caCyt, denoted as paths R3–R6, respectively. As seen from Fig.2, it is already seen that $\bullet\text{OH}$ can form H-bonded complexes with 5-caCyt and hydrogen abstraction reactions may occur from these complexes. The transition states TS3, TS4, TS5, and TS6 corresponding to the abstraction of H3 in IM3, H4 in IM4, H5 in IM5, and H6 in IM6 are located (Fig.6). In all the transition states, the abstractable hydrogen atoms are located closer to the $\bullet\text{OH}$ group associated with ΔG^{\ddagger} values of 54.31, 66.11, 91.90, and $68.89 \text{ kJ}\cdot\text{mol}^{-1}$, respectively, leading to the formation of product radicals P3, P4, P5, and P6. As seen from Table 1 and Fig. 4, the computed results clearly demonstrate that the H4 and H5 abstractions are slightly favored due to thermodynamic control while the H3 and H6 abstractions can only result from kinetic factors.

As seen from Table 2 and Fig. 5, their stabilities are also analyzed by the spin densities. The spin density values of these radical systems are observed mainly on two atoms of 5-caCyt, viz. N3 (0.11) and N4 (0.80) in P3, N3 (0.27) and N4 (0.72) in P4, C5 (0.13) and O4 (0.64) in P6. It may be noted that except P5, all the systems show the partial spin density transferring from $\text{NH}\bullet$ or $\text{COO}\bullet$ group to the pyrimidine ring, resulting in the distortion of the ring plane or $\text{COO}\bullet$ group of 5-caCyt under the influence of the unpaired σ electron. While in the case of P5, the spin density is mainly located on C6 (0.86), indicating a relatively localized unpaired σ electron and an unstable structure in theory. However, the P5 based on the ΔG^{\ddagger} value is the most stable (Table 1). As depicted in Figs. 5 and 6, the geometry of P5 remains a planar character and the ring π -system. The NICS(0) value (-5.82) in the center of the six-membered ring for P5 also shows a strong aromaticity involved the lower energy structure (Table S6). Although path R5 is a strong

exothermic reaction, the ΔG^{\ddagger} value is high, suggesting that path R5 in the gas phase is significant to the disadvantage of the abstraction reaction. Thus in the gas phase, it is obvious that path R4 is much more favorable than other abstraction paths and has a high possibility to occur.

Compared to the addition reaction, the transition states of the abstraction reactions are unstable. The concerned high activation free energies mainly arise from these cyclic transition states. In such cyclic transition states, the orbits required for the bond dissociation and formation are deformed so much that a large amount of deformation energy is substantially needed. Then, it is of great interest whether the activation free energies of the hydrogen abstraction reactions are reduced under strong acid condition. Similarly, what will ensue from the addition reaction? Then, the reaction of $\bullet\text{OH}$ mediated 5-caCyt at a lower pH region has been investigated.

3.1.2 The reaction mechanism of OH-mediated 5-caCytN3⁺

Like in the case of 5-caCyt reaction, the $\bullet\text{OH}$ as a collision partner at a lower pH region results in these paths, the five addition and four hydrogen abstraction reactions, respectively. Similarly, the thermodynamic and kinetic factors both in the gas and aqueous are considered in these reactions (Tables 1 and S7, Fig. S4). Thus, five possible paths for the $\bullet\text{OH}$ -mediated 5-caCytN3⁺ are taken into account in our work, denoted as paths R1', R2', R3', R5', and R6', respectively.

The addition of $\bullet\text{OH}$ to C5 and C6 sites of 5-caCytN3⁺, denoted as paths R1' and R2', respectively (Fig. 7). With approaching $\bullet\text{OH}$ toward the C5 and C6 sites of 5-caCytN3⁺, the complexes IM1' and IM2' are formed. Starting from IM1' and IM2', the $\bullet\text{OH}$ are bonded to C5 and C6 sites of 5-caCytN3⁺ via the transition states TS1' and TS2' with the corresponding ΔG^{\ddagger} values of 34.95 and 48.60 kJ·mol⁻¹, respectively (Fig. 8 and Table 1). Compared to paths R1 and R2, the differences in the structures of the transition states and adduct radicals are very small except for IM1' and IM2'. As for IM1', the interaction between the O of $\bullet\text{OH}$ and the π -face of 5-caCytN3⁺ results in the formation of π -bonded complex, whereas for IM2', the $\bullet\text{OH}$ moved out from the π -face of 5-caCytN3⁺ to the molecular plane eventually leads to the formation of hydrogen bonded complex, thereby exhibiting that there are obvious difference in ΔG^{\ddagger} values. As seen from Table 1, the increase of ΔG^{\ddagger} value is by 32.31~40.48 kJ·mol⁻¹ as compared to those in paths of 5-caCyt, implying that the paths (R1' and R2') are obviously at a disadvantage.

Identify with the abstraction reaction of 5-caCyt, the $\bullet\text{OH}$ is closing to the H3, H5, and H6, respectively, and the corresponding H-bonded complexes IM3', IM5', and IM6' are formed (Fig. 9). And then, the H3, H5, and H6 of 5-caCytN3⁺, respectively, is abstracted via the transition states TS3', TS5', and TS6' with the corresponding ΔG^{\ddagger} values of 88.69, 77.10, and 64.73 kJ·mol⁻¹, respectively (Figs. 8 and 9). This suggests that path R6', relative to paths R3' and R5', is likely to happen in the gas phase.

As seen from Table 1, it is obvious that the $\bullet\text{OH}$ addition reactions at a lower pH range have smaller activation free energies with the range of 16.13~53.74 kJ·mol⁻¹ than those of the hydrogen abstraction reaction, suggesting that the reactivity of $\bullet\text{OH}$ with 5-caCytN3⁺ is actually dominated

by addition. However, the ΔG^{\ddagger} values of $\bullet\text{OH}$ -mediated 5-caCyt paths are higher in strong acid condition than in neutral condition, and then, it is of great concern whether the ΔG^{\ddagger} values of these paths will be influenced in alkaline surrounding.

3.1.3 The reaction mechanism of OH-mediated 5-caCytCOO⁻

The $\bullet\text{OH}$ -mediated 5-caCyt in alkaline surrounding is described as alkaline-induced process by the similar way as neutral and acid conditions, named as R1"~R5", respectively. Indentify with the reactions in neutral and acid conditions, the alkaline-induced processes are starting from these complexes IM1"~IM5" associated with the transition states TS1" ~TS5" with the corresponding ΔG^{\ddagger} values of 32.31, 17.29, 51.09, 87.06, and 30.65 kJ·mol⁻¹, respectively (Figs.10-12 and Table 1). The structures of transition states and product radicals formed in alkaline condition are similar as those in neutral and acid conditions, whereas these complexes formed have great difference except for IM3", which results from the strong interaction between COO⁻ and H of $\bullet\text{OH}$. These lead to the difference of ΔG^{\ddagger} . As seen from Table 1, two addition and H-atom abstraction (H3 and H5) are primarily controlled by thermodynamic factors, while the abstraction of H4 is mainly controlled by weak kinetic factors. Table 1 also illustrates that alkaline, relative to the neutral condition, has negative catalysis for the addition reaction, whereas has positive catalysis for the H5 atom abstraction.

As mentioned above, the ΔG^{\ddagger} values of $\bullet\text{OH}$ -mediated 5-caCyt are to some degree affected by the acid-base environment. Then, it is of great interest whether the ΔG^{\ddagger} values of these paths are further influenced by the contribution of the bulk water.

3.2 Stationary point structures and energetics in the aqueous phase

In modeling solvation effects, an important question arises as to whether computational results are sensitive to the presence of the bulk water. The solvation effect on the $\bullet\text{OH}$ -mediated 5-caCyt, 5-caCytN3⁺, and 5-CytCOO⁻, respectively, has been discussed. The important bond lengths of all stationary points for all paths in the aqueous phase are also shown in Figs.S5-S13, implying that the small geometrical changes are induced by the presence of the bulk water. The influence of solvation on the activation free energies can be explained by the evolution of the dipole moments for all paths (Table 3).

As for in neutral condition, the activation free energy of path R3 in water is 11.94 kJ·mol⁻¹ higher than in the gas phase, attributed to that the dipole moment of TS3 ($\mu=5.46$ debye) is much less than that of IM3 ($\mu= 8.60$ debye), and the transition state TS3 is unstabilized in water by solvation. This indicates water has a significantly negative catalytic effect on path R3. Dissimilar with path R3, the dipole moments ($\mu=6.63$ debye for TS5 and 8.28 debye for TS6) are larger than their intermediates ($\mu=5.74$ debye for IM5 and 4.27 debye for IM6), and then the solvation of water on their transition states are stronger than on intermediates. This can explain why the paths R5 and R6 are associated with lower activation free energies in the aqueous phase than in the gas phase, illustrating that water has a positive catalytic effect on these paths. And for R1 and R2, the dipole moments of TS1 and TS2, relative to IM1 and IM2, have very small change by about

0.13~0.44 debye, indicating that solvation is comparatively negligible.

Note that water has also a significantly negative catalytic effect on path R4. But unlike R3, the dipole moment ($\mu=7.61$ debye for TS4) is a little bit larger than its intermediate ($\mu=7.17$ debye for IM4), suggesting that the solvation of water on its transition state is a little stronger than on intermediate. By that analogy, the activation free energy of path R4 should be a bit lower in the aqueous phase than in the gas phase. However, the dipole moment approach obviously appears to fail. For this reason, the NPA charges are introduced. The O of $\bullet\text{OH}$ has strong electronegativity, and the increase of negative charge for the oxygen atom shows high reactivity toward the hydrogen donor. The present computed NPA charges on O of $\bullet\text{OH}$ for IM4 in the gas and aqueous phases are -0.415 and 0.287 e, respectively (Table S8), which may explain that why the path R4 in the aqueous phase is associated with poorer reaction trend than in the gas phase.

As for in strong acid condition, the solvation have more or less effect on the $\bullet\text{OH}$ -mediated 5-caCytN3⁺. The activation free energies of paths R1'~R3', R5' and R6', are reduced from 34.95, 48.60, 88.69, 77.10, and 64.73 kJ·mol⁻¹ to 17.55, 31.97, 87.66, 57.53, and 61.28 kJ·mol⁻¹, respectively, illustrating that water have positive catalytic effect on these paths. The same conclusion is obtained from the evolution of the dipole moments. As for in alkaline condition, the solvation still have to some extent effect on the $\bullet\text{OH}$ -mediated 5-CytCOO⁻. The ΔG^{\ddagger} values of paths R1''~R5'' are 12.18, 15.74, 63.32, 91.26, and 32.55 kJ·mol⁻¹, illustrating that water have positive catalytic effect on the addition reaction, whereas the solvation effect is reversed for the H5 atom abstraction.

As seen from Table 1, as for the addition, 5-caCyt shows nearly barrierless for the C5 channel and a small barrier of 11.99 kJ·mol⁻¹ for the C6 route. Similarly, the observed small difference also exists in 5-caCytN3⁺ and 5-CytCOO⁻ paths. These results indicate some amount of regioselectivity, which agrees with the tendencies found experimentally.¹⁹ As for the abstraction reaction, the H5 atom is easier to be abstracted in neutral, acid and alkaline conditions. Moreover, the H5 abstraction in alkaline media might be competitive with the addition reactions, having a ΔG^{\ddagger} value of 32.55 kJ·mol⁻¹, which is only 17-20 kJ·mol⁻¹ more energetic than the results for the addition reactions.

4. Summary and conclusions

Three distinct groups of $\bullet\text{OH}$ -mediated 5-caCyt mechanisms have been explored in this work, the direct reaction (paths R1~R6), the acid-induced process (paths R1'~R3', R5' and R6'), and the alkaline-catalytic reaction (paths R1''~R5''), respectively. Meanwhile, these paths have been further investigated by the contribution of the bulk water.

(1) The addition of $\bullet\text{OH}$ to the C5=C6 double bond of 5-caCyt is the most favourable in neutral, acid and alkaline conditions, and the ΔG^{\ddagger} value of C5 channel is a little higher than that of C6 route. The observed small differences in the activation free barriers indicate some amount of regioselectivity,^{15g-1,44} which also agrees with the tendencies found experimentally.¹⁹ This is also in agreement with the conclusions of $\bullet\text{OH}$ -mediated cytosine reaction reported by experimentally

and theoretically.⁴⁵

(2) The differences of ΔG^{\ddagger} values for the $\bullet\text{OH}$ addition to neutral, deprotonated and N3-protonated 5-caCyt are small, implying that the discrimination is not obviously from an energetic point of view. The ΔG^{\ddagger} values of N3-protonated 5-caCyt system are slightly higher, indicating that the reaction trends are a little weakened.

(3) Concerning the H-atom abstractions, the H5 atom at the C6 position seems to be more labile than abstraction at other positions in neutral, acid and alkaline conditions. Moreover, the H5 abstraction in alkaline media might be competitive with the addition reactions, having a ΔG^{\ddagger} value of $32.55 \text{ kJ}\cdot\text{mol}^{-1}$, which is only $17\text{-}20 \text{ kJ}\cdot\text{mol}^{-1}$ more energetic than for the addition reactions. As far as we know, this is firstly theoretical report unveiling the effect of acid-base environment in radical reactions, which is also likely to be a new insight for the reactivity of nucleosides with a hydroxyl radical.

5. Final Remarks

As seen from Table 1, the addition to the C5=C6 double bond is more favourable. Concerning the H-atom abstractions, the H atom at the C6 position seems to be more labile than abstraction at other positions according to the present results. Meanwhile, it is clear that the addition and H5 atom abstraction for 5-caCyt are prone to happen in neutral or alkaline media, suggesting that the DNA bases are easily damaged when exposed the surrounding of hydroxyl radicals in such case. On the contrary, the reaction trend of $\bullet\text{OH}$ -mediated 5-caCyt is somewhat weakened at very lower pH. Moreover, the product radical formed by 5-caCyt and $\bullet\text{OH}$ in the aqueous phase is less stable in acid condition than in neutral and alkaline conditions, hinting that it is not necessary to decompose these product radicals in harsh condition. Then DNA bases may be relieved from oxidation at low pH. The 5-caCyt at the N3 position is easily protonated at $\text{pH} < 1$. However, the DNA macromolecule should be hydrolysed in this strongly acidic pH, even at milder conditions. Therefore, some protective measures for DNA bases should be taken. For example, some antioxidants should be added in mammalian brain tissues. The reason is that the many antioxidants that can protect biomolecules against DNA damage. However, antioxidant protection against free radicals should be taken with caution since the antioxidant action might actually stimulate cancer progression through the enhanced survival of tumour cells. Of course it would be better to avoid all the radicals for DNA bases. This work might provide some implications for clarifying the reason of these diseases caused by $\bullet\text{OH}$ mediated damage to biomolecules.

Acknowledgment

This work was supported by the National Natural Science Foundation of China (No: 21473108), Shaanxi Innovative Team of Key Science and Technology (2013KCT-17), and the introducing talents Foundation of Shaanxi University of Technology (No: SLGKYQD2-13, SLGQD14-10).

References

- (1) J. A. Theruvathu, C. T. Aravindakumar, R. Flyunt, J. von Sonntag and C. von Sonntag, *J. Am. Chem. Soc.*, 2001, **123**, 9007.
- (2) Q. Y. Cheng, J. D. Gu, K. R. Compaan and H. F. Schaefer, *Chem. Eur. J.*, 2010, **16**, 11848.
- (3) T. Finkel and N. J. Holbrook, *Nature*, 2000, **408**, 239;
- (4) B. N. Ames, M. K. Shigenaga and T. M. Hagen, *Proc. Natl. Acad. Sci. USA*, 1993, **90**, 7915.
- (5) V. K. C. Ponnaluri, J. P. Maciejewski and M. Mukherji, *Biochem. Biophys. Res. Commun.*, 2013, **436**, 115.
- (6) H. Zhao and T. Chen, *J. Hum. Genet.*, 2013, **58**, 421.
- (7) L. Shen and Y. Zhang, *Curr. Opin. Cell. Biol.*, 2013, **25**, 289.
- (8) S. Schiesser, B. Hackner, T. Pfaffeneder, M. Müller, C. Hagemeyer, M. Truss and T. Carell, *Angew. Chem. Int. Ed.*, 2012, **51**, 6516.
- (9) C. P. Walsh, G. L. Xu and Curr. Top, *Microbiol. Immunol.*, 2006, **301**, 283.
- (10) C. G. Spruijt, F. Gnerlich, A. H. Smits, T. Pfaffeneder, P. W. T. C. Jansen, C. Bauer, M. Münzel, M. Wagner, M. Müller, F. Khan, H. C. Eberl, A. Mensinga, A. B. Brinkman, K. Lephikov, U. Müller, J. Walter, R. Boelens, H. van Ingen, H. Leonhardt, T. Carell and M. Vermeulen, *Cell*, 2013, **152**, 1146.
- (11) M. W. Kellinger, C. X. Song, J. Chong, X. Y. Lu, C. He and D. Wang, *Nat. Struct. Mol. Biol.*, 2012, **19**, 831.
- (12) X. W. Xing, Y. L. Liu, M. Vargas, Y. Wang, Y. Q. Feng, X. Zhou and B. F. Yuan, *PLoS One.*, 2013, **8**, 8e72993.
- (13) H. Wu and Y. Zhang, *Cell*, 2014, **156**, 45.
- (14) M. Valko, M. Izakovic, M. Mazur, C. J. Rhodes and J. Telser, *Mol. Cell. Biochem.*, 2004, **266**, 37.
- (15) a) C. J. Burrows and J. G. Muller, *Chem. Rev.*, 1998, **98**, 1109.; b) J. Cadet, M. Berger, T. Douki and J. L. Ravanat, *Rev. Physiol. Biochem. Pharmacol.*, 1997, **131**, 1.; c) W. K. Pogozelski and T. D. Tullius, *Chem. Rev.*, 1998, **98**, 1089.; d) J. R. Wagner, C. Decarroz, M. Berger and J. Cadet, *J. Am. Chem. Soc.*, 1999, **121**, 4101.; e) J. Cadet, T. Douki and J. L. Ravanat, *Acc. Chem. Res.*, 2008, **41**, 1075.; f) G. Pratviel and B. Meunier, *Chem. Eur. J.*, 2006, **12**, 6018.; g) J. R. Wagner and J. Cadet, *Acc. Chem. Res.*, 2010, **43**, 564.; h) Y. J. Ji and Y. Y. Xia, *Int. J. Quantum Chem.*, 2005, **101**, 211.; i) F. M. Antonio, M. Manuela and R. S. Daniel, *J. Phys. Chem. B.*, 2014, **118**, 2932.; l) A. Adhikary, A. Kumar, A. N. Heizer, B. J. Palmer, V. Pottiboyina, Y. Liang.; S. F. Wnuk and M. D. Sevilla, *J. Am. Chem. Soc.*, 2013, **135**, 3121.
- (16) a) J. Cadet, T. Delatour, T. Douki, D. Gasparutto, J. P. Pouget, J. L. Ravanat and S. Sauvaigo, *Mutat. Res.*, 1999, **424**, 9.; b) C. Chatgililoglu, M. D. Angelantonio, M. Guerra, P. Kaloudis and Q. G. Mulazzani, *Angew. Chem.*, 2009, **121**, 2248.
- (17) S. Zuo, R. J. Boorstein and G. W. Teebor, *Nucleic Acids Res.*, 1995, **23**, 3239.
- (18) C. Von. Sonntag, Taylor & Francis, London. 1987.
- (19) D. K. Hazra and S. Steenken, *J. Am. Chem. Soc.*, 1983, **105**, 4380.
- (20) M. Sumino, A. Ohkubo, H. Taguchi, K. Seio and M. Sekine, *Bioorg. Med. Chem. Lett.*, 2008, **18**, 274.
- (21) S. Irrera and G. Portalone, *J. Mol. Struct.*, 2013, **1050**, 140.
- (22) A. Maiti, A. Z. Michelson, C. J. Armwood, J. K. Lee and A. C. Drohat, *J. Am. Chem. Soc.*, 2013, **135**, 15813.
- (23) M. Chen and J. K. Lee, *J. Org. Chem.*, 2014, **79**, 11295.
- (24) Z. A. Shabarova and A. A. Bogdanov, *Advanced Organic Chemistry of Nucleic Acids*, Wiley, 1994, p185.
- (25) M. J. Frisch, G. W. Trucks, H. B. Schlegel, G. E. Scuseria, M. A. Robb, J. R. Cheeseman, G. Scalmani, V. Barone, B. Mennucci, G. A. Petersson, H. Nakatsuji, M. Caricato, X. Li, H. P. Hratchian, A. F. Izmaylov, J. Bloino, G. J. Zheng, L. Sonnenberg, M. Hada, M. Ehara, K. Toyota, R. Fukuda, J. Hasegawa, M. Ishida, T. Nakajima, Y. Honda, O. Kitao, H. Nakai, T. Vreven, J. J. A. Montgomery, J. E. Peralta, F. Ogliaro, M. Bearpark, J. J. Heyd, E. Brothers, K. N. Kudin, V. N. Staroverov, R. Kobayashi, J. Normand, K. Raghavachari, A. Rendell, J. C. Burant, S. S. Iyengar, J. Tomasi, M. Cossi, N. Rega, J. M. Millam, M. Klene, J. E. Knox, J. B. Cross, V. Bakken, C. Adamo, J.

Jaramillo, R. Gomperts, R. E. Stratmann, O. Yazyev, A. J. Austin, R. Cammi, C. Pomelli, J. W. Ochterski, R. L. Martin, K. Morokuma, V. G. Zakrzewski, G. A. Voth, P. Salvador, J. J. Dannenberg, S. Dapprich, A. D. Daniels, O. Farkas, J. B. Foresman, J.V. Ortiz, J. Cioslowski,; D. J. Fox, Gaussian 09, Revision A.02. Gaussian, Inc., Wallingford, CT, **2009**.

- (26) J. A. Montgomery, M. J. Frisch, J. W. Ochterski and G. A. Petersson, *J. Chem. Phys.*, 1999, **110**, 2822.
- (27) A. G. Baboul, L. A. Curtiss, P. C. Redfern and K. Raghavachari, *J. Chem. Phys.*, 1999, **110**, 7650.
- (28) B. Sirjean and R. Fournet, *J. Phys. Chem. A*, 2012, **116**, 6675.
- (29) B. Sirjean, P. A. Glaude, M. F. Ruiz-López and R. Fournet, *J. Phys. Chem. A*, 2006, **110**, 12693.
- (30) B. Sirjean, P. A. Glaude, M. F. Ruiz-López and R. Fournet, *J. Phys. Chem. A*, 2009, 113, 6924.
- (31) E. K. Pokon, M. D. Liptak, S. Feldgus and G. C. Shields, *J. Phys. Chem. A*, 2001, **105**, 10483.
- (32) J. W. Ochterski, G. A. Petersson and J. A. Montgomery Jr, *J. Chem. Phys.* 1996, **104**, 2598.
- (33) M. R. Nyden, G. A. Petersson, *J. Chem. Phys.*, 1981, **75**, 1843.
- (34) G. A. Petersson, A. Bennett, T. G. Tensfeld, M. A. Al-Laham, W. Shirley and J. Matzaris, *J. Chem. Phys.*, 1988, **89**, 2193.
- (35) G. A. Petersson and M. A. Al-Laham, *J. Chem. Phys.*, 1991, **94**, 6081.
- (36) G. A. Petersson, A. K. Yee and A. Bennett, *J. Chem. Phys.*, 1985, **83**, 5105.
- (37) J. A. Montgomery, J. W. Ochterski and G. A. Petersson, *J. Chem. Phys.*, 1994, **101**, 5900.
- (38) W. J. Hehre, R. Ditchfield and J. A. Pople, *J. Chem. Phys.*, 1972, **56**, 2257.
- (39) E. Cancès, B. Mennucci, and J. Tomasi, *J. Chem. Phys.*, 1997, **107**, 3032.
- (40) a) B. Ośmiałowski, E. Kolehmainen and R. Gawinecki, *Magn. Reson. Chem.*, 2001, **39**, 334.; b) M. Szafran, A. Komasa, A. Katrusiak, Z. Dega-Szafran and P. Barczyński. *J. Mol. Struct.*, 2007, **844**, 102.; c) M. Senyel, O. Alver and C. Parlak, *Spectrochim. Acta A*, 2008, **71**, 830.; d) A. R. Katritzky, N. G. Akhmedov, J. Doskocz, C. D. Hall, R. G. Akhmedova and S. Majumder, *Magn. Reson. Chem.*, 2007, **45**, 5.; e) C. Parlak, O. Alver and M. Senyel, *Spectrochim. Acta A: Mol. Biomol. Spectrosc.*, 2008, **69**, 1252.; f) A. R. Katritzky, N. G. Akhmedov, J. Doskocz, P. P. Mohapatra and C. D. Hall, *A. Güven, Magn. Reson. Chem.*, 2007, **45**, 532.
- (41) A. E. Reed, R. B. Weinstock and F. Weinhold, *J. Chem. Phys.*, 1985, **83**, 735.
- (42) A. E. Reed, L. A. Curtiss and F. Weinhold, *Chem. Rev.*, 1988, **88**, 899.
- (43) W. W. Cleland and M. M. Kreevoy, *Science*, 1994, **264**, 1887.
- (44) a) K. P. Prasanthkumar, C. H. Suresh and C. T. Aravindakumar, *Radiat. Phys. Chem.*, 2012, **81**, 267.; b) S. Naumov and C. von Sonntag, *Radiat. Res.*, 2008, **169**, 355.
- (45) S. V. Jovanovic and M. G. Simic, *J. Am. Chem. Soc.*, 1986, **108**, 5968.

Table content:**Table 1** Relative Energies ^a (kJ·mol⁻¹) for the Reaction of •OH-mediated 5-caCyt, 5-caCytN3⁺ and 5-caCytCOO⁻ Both in the Gas and Aqueous Phases

System	Species	CBS-QB3 ^b			PCM ^c	
		ΔE^g	ΔG^g	$\Delta G^{g\ddagger}$	$\Delta G^{g\ddagger}$	
Addition Reactions						
Reactions of •OH-mediated 5-caCyt	R ^d	0.00	0.00		0.00	
	IM1	-7.68	23.12		27.76	
	TS1	-11.71	25.76		28.64	
	P1	-51.39	-14.22		-6.84	
	IM2	-12.54	19.56		28.27	
	TS2	-11.47	27.68		40.26	
	P2	-92.61	-55.84		-42.00	
	IM1→P1			2.64	0.88	
	IM2→P2			8.12	11.99	
	H-atom Abstraction Reactions					
	IM3	-27.18	4.60		12.80	
	TS3	22.04	58.91		79.05	
	P3	-20.80	9.70		-15.23	
	IM4	-14.29	14.35		16.22	
	TS4	44.49	80.46		99.23	
	P4	-28.89	1.39		1.51	
	IM5	-8.56	20.75		27.25	
	TS5	24.12	112.65		66.67	
P5	-31.77	-6.90		-11.53		
IM6	-28.44	5.69		19.83		
TS6	40.45	74.57		72.99		
P6	-16.48	15.21		-22.36		
IM3→P3			54.31	66.25		
IM4→P4			66.11	83.01		
IM5→P5			91.90	39.42		
IM6→P6			68.89	53.16		
Addition Reactions						
Reactions of •OH-mediated 5-caCytN3 ⁺	R ^e	0.00	0.00		0.00	
	IM1'	-27.85	-2.54		23.75	
	TS1'	-4.73	32.41		41.30	
	P1'	-53.70	-15.61		-2.97	
	IM2'	-34.81	-8.46		17.03	
	TS2'	1.65	40.14		49.00	
	P2'	-79.17	-41.47		-39.20	
	IM1'→P1'			34.95	17.55	
	IM2'→P2'			48.60	31.97	
	H-atom Abstraction Reactions					
IM3'	-44.59	-14.00		16.15		
TS3'	38.77	74.69		103.81		
P3'	-47.17	-23.31		-2.34		
IM5'	-34.81	-8.45		23.35		

	TS5'	36.23	68.65	80.88	
	P5'	-59.13	-34.18	-2.83	
	IM6'	-31.74	-4.61	17.70	
	TS6'	25.01	60.12	78.98	
	P6'	42.17	-325.88	37.74	
	IM3'→P3'			88.69	87.66
	IM5'→P5'			77.10	57.53
	IM6'→P6'			64.73	61.28
	Addition Reactions				
	R ^f	0.00	0.00	0.00	
	IM1''	-60.31	-27.01	6.35	
	TS1''	-35.43	5.30	18.53	
	P1''	-93.21	-53.11	-35.78	
	IM2''	-60.31	-27.01	6.35	
	TS2''	-41.15	-9.72	22.09	
	P2''	-116.60	-78.56	-59.65	
	IM1''→P1''			32.31	12.18
	IM2''→P2''			17.29	15.74
	H-atom Abstraction Reactions				
Reactions of •OH-mediated 5-caCytCOO ⁻	IM3''	-53.37	-18.05	4.68	
	TS3''	-5.49	33.04	68.00	
	P3''	-86.49	-55.01	-30.08	
	IM4''	-60.73	-29.30	-2.02	
	TS4''	19.61	57.76	89.24	
	P4''	-44.29	-14.21	1.24	
	IM5''	-60.31	-27.01	6.35	
	TS5''	-31.11	3.64	38.90	
	P5''	-65.24	-36.44	-13.68	
	IM3''→P3''			51.09	63.32
	IM4''→P4''			87.06	91.26
IM5''→P5''			30.65	32.55	

^a ΔE^{\ddagger} , ΔG^{\ddagger} , and $\Delta G^{\ddagger\ddagger}$ are relative energy, relative free energy, and activation free energy in the gas phase, respectively; ΔG° and $\Delta G^{\circ\ddagger}$ are relative free energy and activation free energy with PCM model based on the optimized geometries in the aqueous phase. ^b CBS-QB3 composite approach. ^c CBS-QB3 with PCM model. ^d denotes 5-caCyt+•OH. ^e denotes 5-caCytN3⁺+•OH. ^f denotes 5-CytCOO⁻+•OH.

Table 2 The Partial Atomic Spin Densities in the Gas Phase for the Product Radicals of •OH-mediated 5-caCyt

Species	P1	P2	P3	P4	P5	P6
N1	0.14					
O1			0.13			0.20
O2	0.11	0.11				
N3		0.24	0.11	0.27		
C4		-0.11	-0.17	-0.12		
N4			0.80	0.72		
C5		0.72				0.13
C6	0.64				0.86	
C7						
O3		0.13				
O4						0.64

Table 3 The Evolution of the Dipole Moments (μ , in Debye) for the Reactions of $\bullet\text{OH}$ -mediated 5-caCyt (R1~R6), 5-caCytN3⁺ (R1'~R3', R5', R6'), and 5-CytCOO⁻ (R1''~R5'')

Reactions of $\bullet\text{OH}$ -mediated 5-caCyt											
R1	μ	R2	μ	R3	μ	R4	μ	R5	μ	R6	μ
IM1	7.32	IM2	4.82	IM3	8.60	IM4	7.17	IM5	5.74	IM6	4.27
TS1	6.88	TS2	4.95	TS3	5.46	TS4	7.61	TS5	6.63	TS6	8.28
Reactions of $\bullet\text{OH}$ -mediated 5-caCytN3 ⁺											
R1'	μ	R2'	μ	R3'	μ	--	--	R5'	μ	R6'	μ
IM1'	1.11	IM2'	0.79	IM3'	0.99	--	--	IM5'	0.79	IM6'	2.09
TS1'	1.56	TS2'	1.29	TS3'	2.86	--	--	TS5'	2.16	TS6'	2.80
Reactions of $\bullet\text{OH}$ mediated 5-CytCOO ⁻											
R1''	μ	R2''	μ	R3''	μ	R4''	μ	R5''	μ	--	--
IM1''	2.53	IM2''	2.53	IM3''	3.73	IM4''	4.75	IM5''	2.53	--	--
TS1''	2.82	TS2''	2.65	TS3''	4.73	TS4''	4.35	TS5''	2.82	--	--

Captions:

Fig. 1 Prevailing species of the 5-caCyt moiety in 5-carboxyl-2'-deoxycytidine (H7 =2'-deoxyribose) at different pH: (a) at pH < 1, (b) and (c) at pH = 2~ 9 [21].

Fig. 2 Optimized structures (bond distances in Å) of the H-bonded and π -bonded complexes for •OH-mediated 5-caCyt in the gas phase at the CBS-QB3 composite approach.

Fig. 3 Optimized structures (bond distances in Å) in the gas phase for the addition reaction of •OH-mediated 5-caCyt (paths R1 and R2) at the CBS-QB3 composite approach.

Fig. 4 The potential energy surfaces (ΔG^\ddagger in $\text{kJ}\cdot\text{mol}^{-1}$) along the reaction of •OH-mediated 5-caCyt (paths R1-R6) in the gas phase. R denotes 5-caCyt +•OH.

Fig. 5 The map of spin densities distribution for the product radicals of the •OH-mediated 5-caCyt in the gas phase.

Fig. 6 Optimized structures (bond distances in Å) in the gas phase for the H-atom abstraction reaction of •OH-mediated 5-caCyt (paths R3-R6) at the CBS-QB3 composite approach.

Fig. 7 Optimized structures (bond distances in Å) in the gas phase for the addition reaction of •OH-mediated 5-caCytN3⁺ (paths R1' and R2') at the CBS-QB3 composite approach.

Fig. 8 The potential energy surfaces (ΔG^\ddagger in $\text{kJ}\cdot\text{mol}^{-1}$) along the reaction of •OH-mediated 5-caCytN3⁺ (paths R1'~R3', R5' and R6') in the gas phase. R' denotes 5-caCytN3⁺ +•OH.

Fig. 9 Optimized structures (bond distances in Å) in the gas phase for the H-atom abstraction reaction of •OH-mediated 5-caCytN3⁺ (paths R3', R5', and R6') at the CBS-QB3 composite approach.

Fig. 10 Optimized structures (bond distances in Å) in the gas phase for the addition reaction of •OH-mediated 5-CytCOO⁻ (paths R1'' and R2'') at the CBS-QB3 composite approach.

Fig. 11 The potential energy surfaces (ΔG^\ddagger in $\text{kJ}\cdot\text{mol}^{-1}$) along the reaction of •OH-mediated 5-CytCOO⁻ (paths R1''~R5'') in the gas phase. R'' denotes 5-CytCOO⁻ +•OH.

Fig. 12 Optimized structures (bond distances in Å) in the gas phase for the H-atom abstraction reaction of •OH-mediated 5-CytCOO⁻ (paths R3''~R5'') at the CBS-QB3 composite approach.

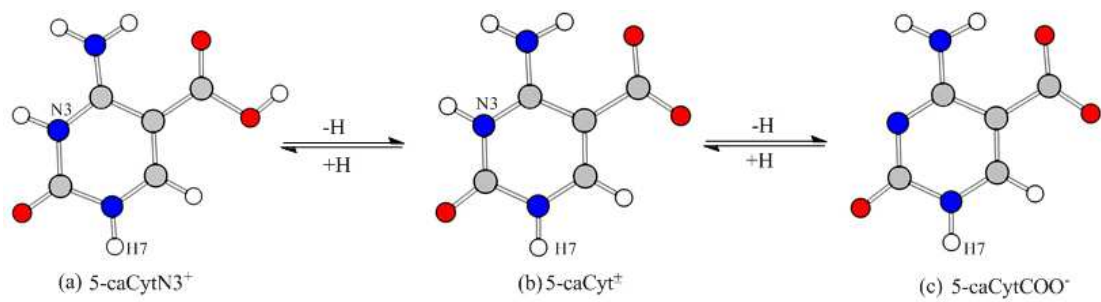


Fig.1

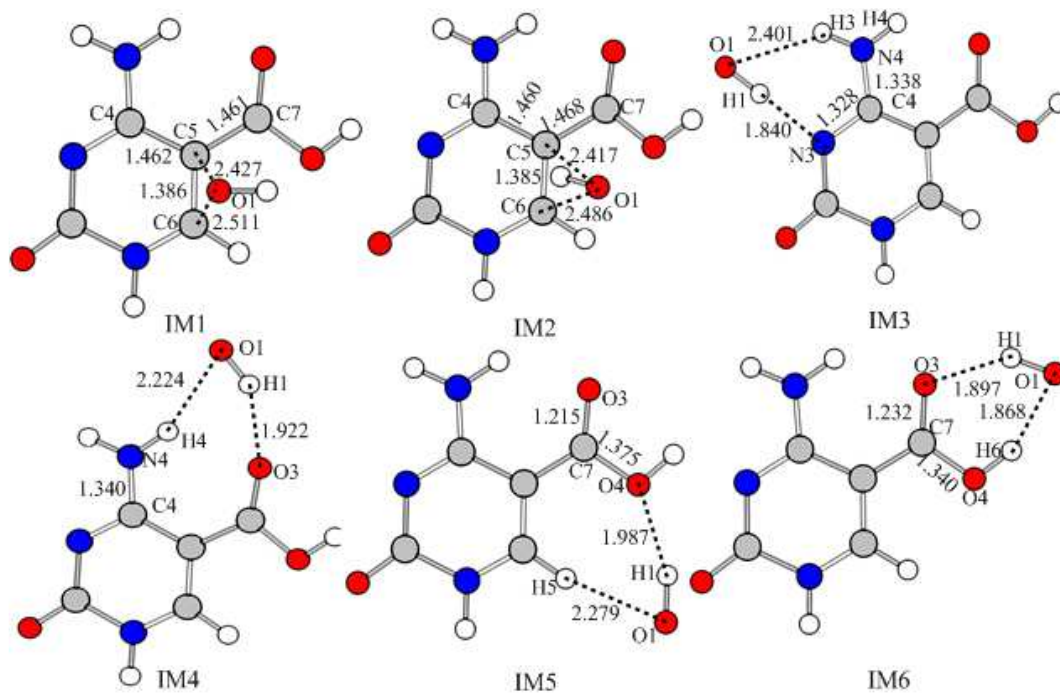


Fig.2

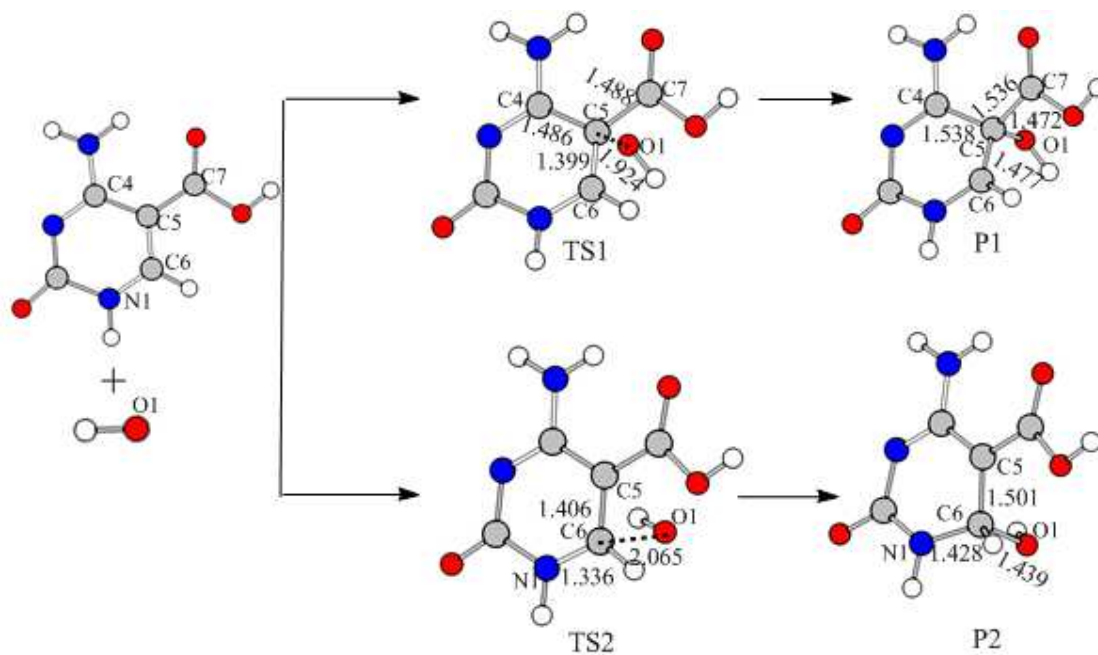


Fig.3

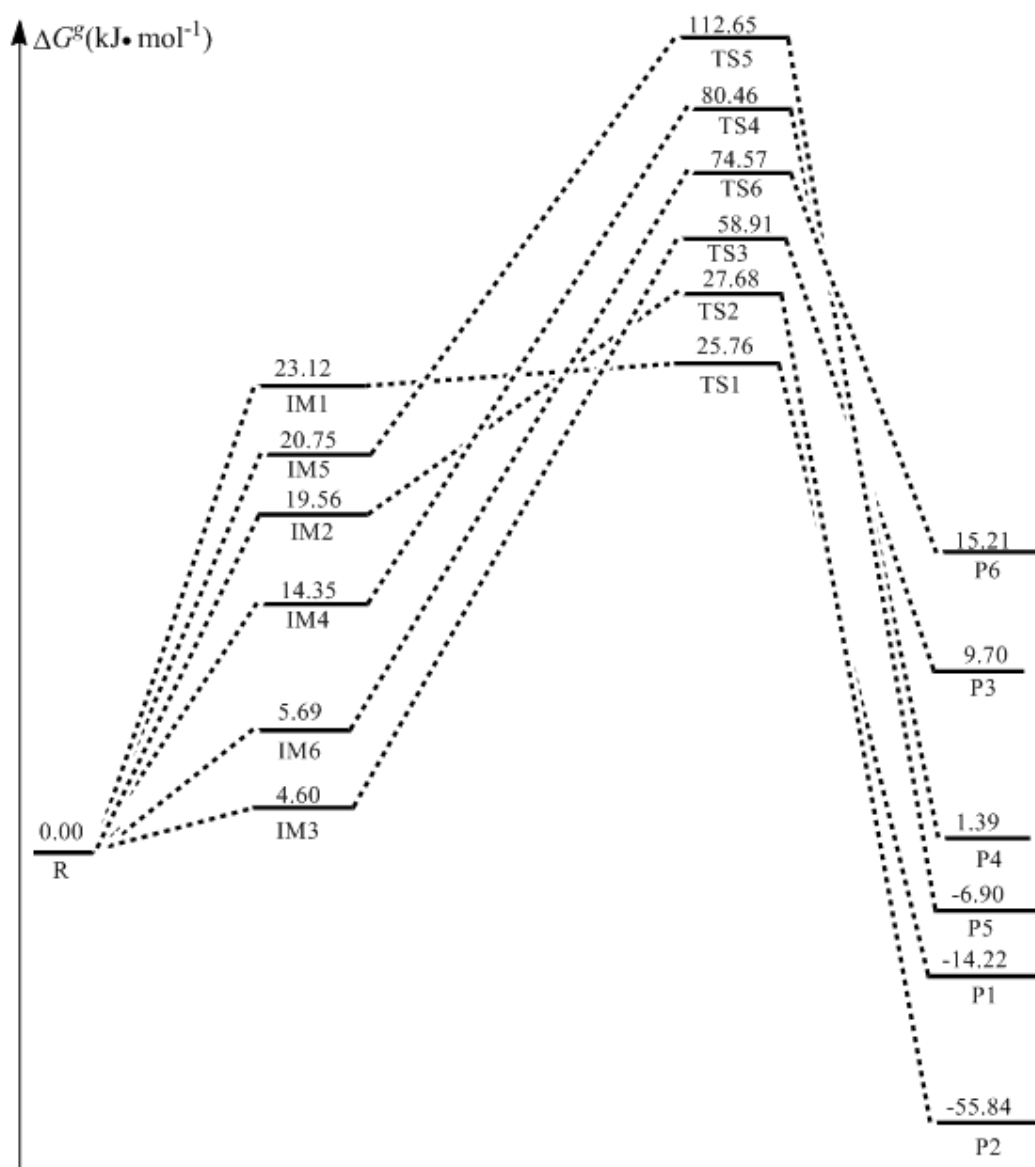


Fig.4

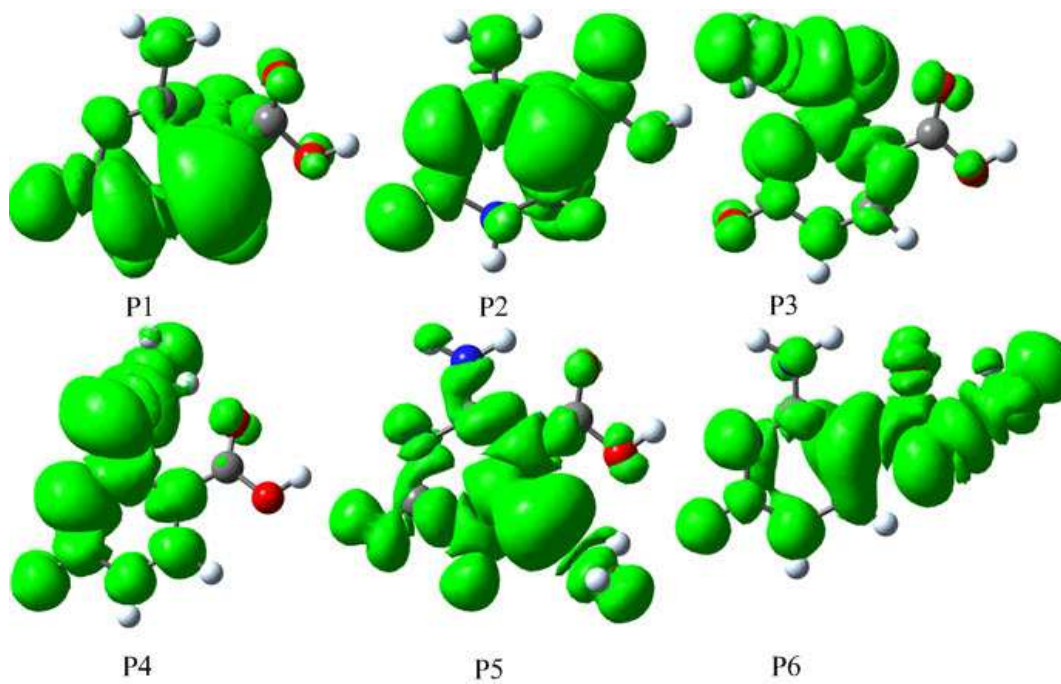


Fig.5

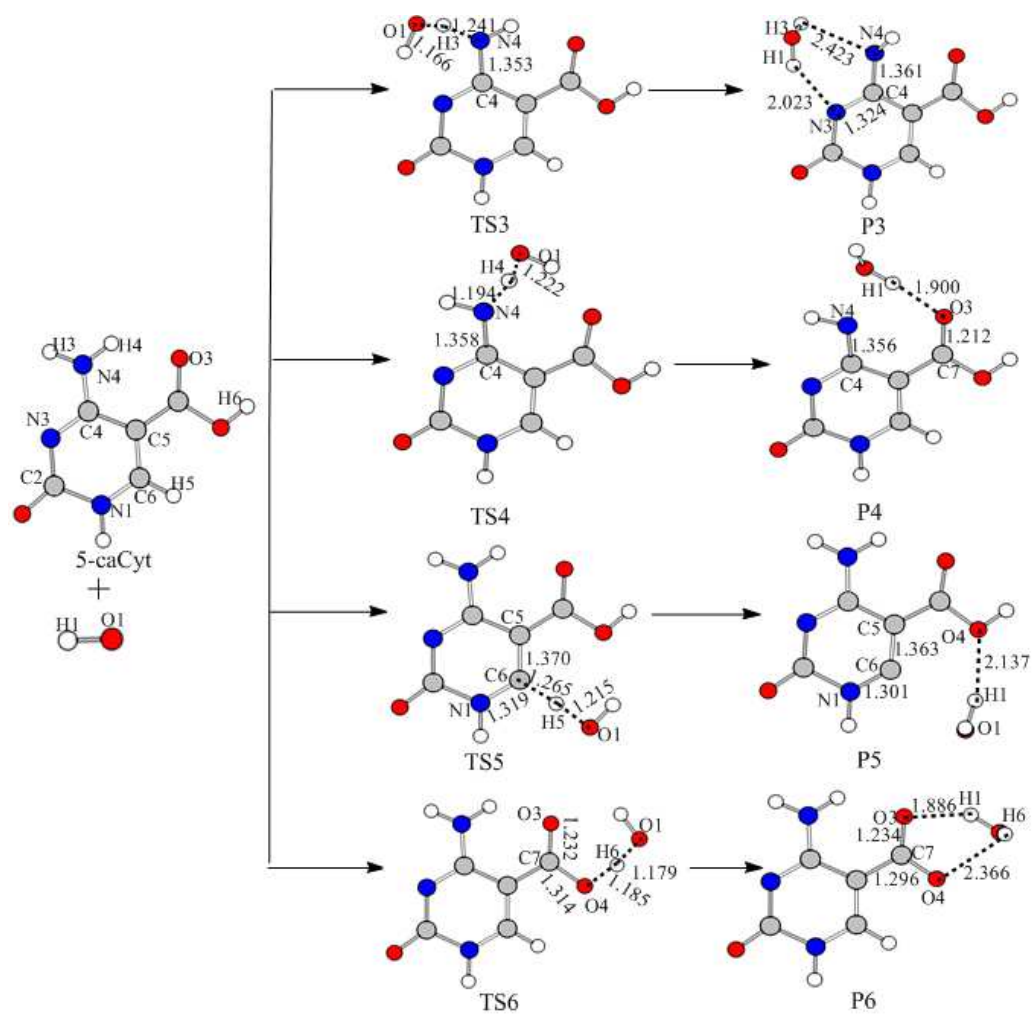


Fig.6

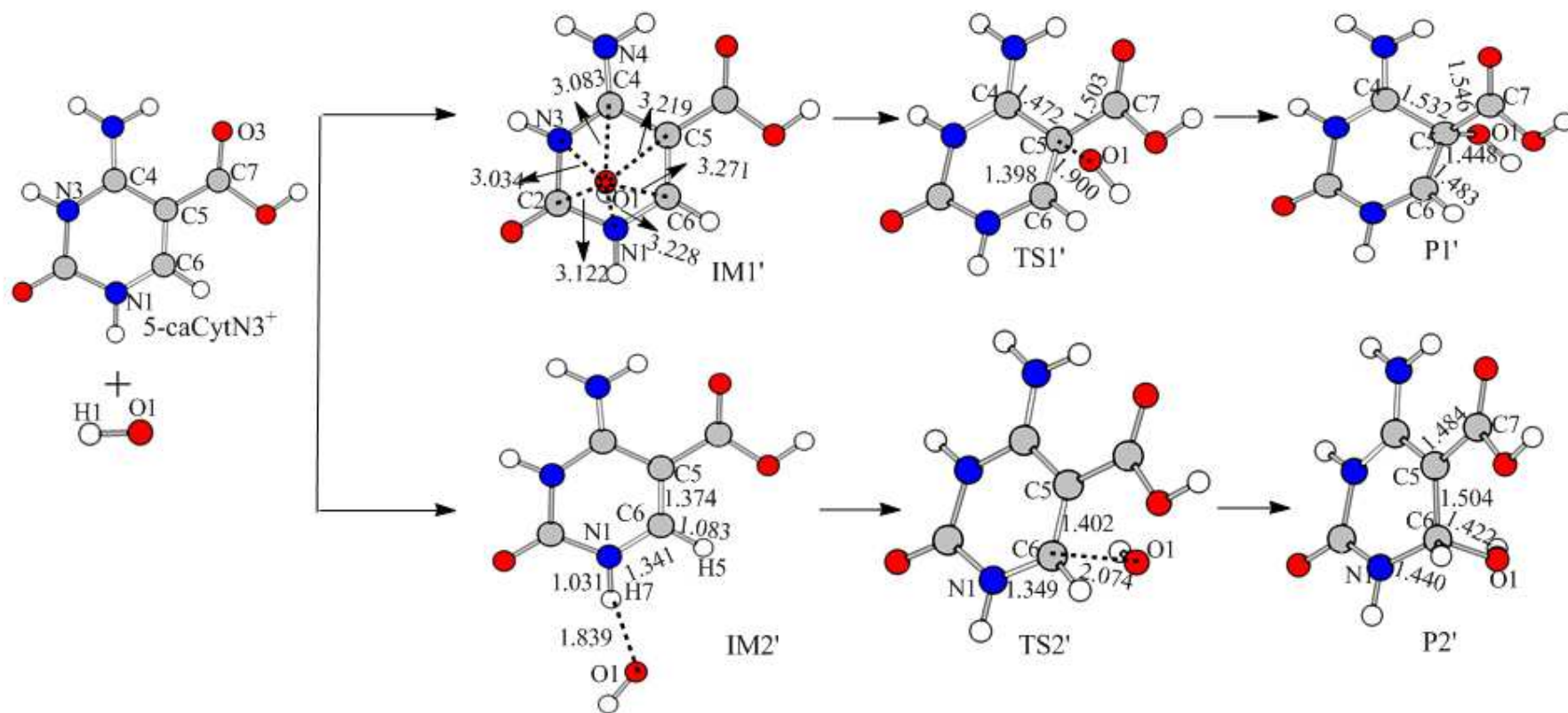


Fig.7

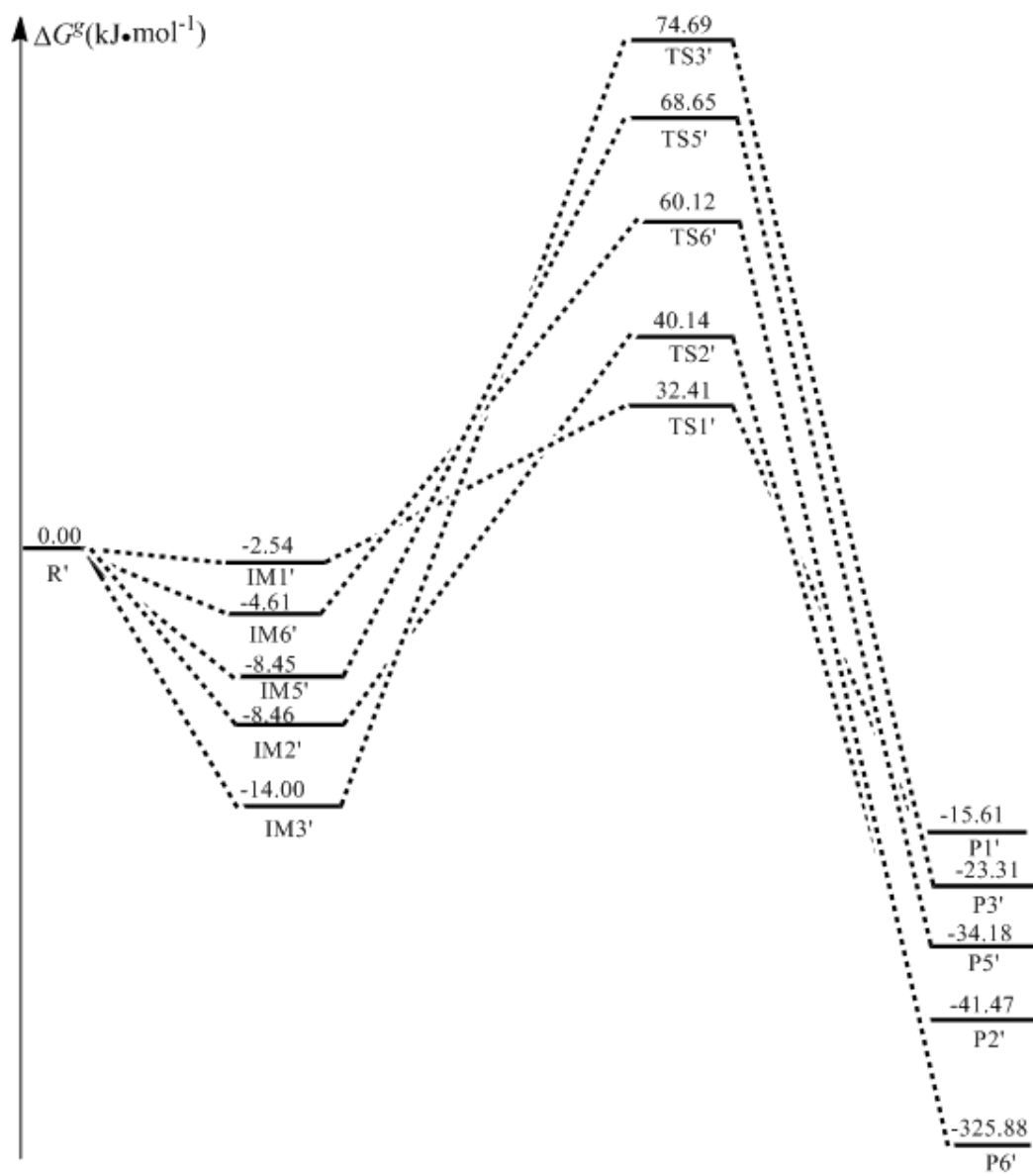


Fig.8

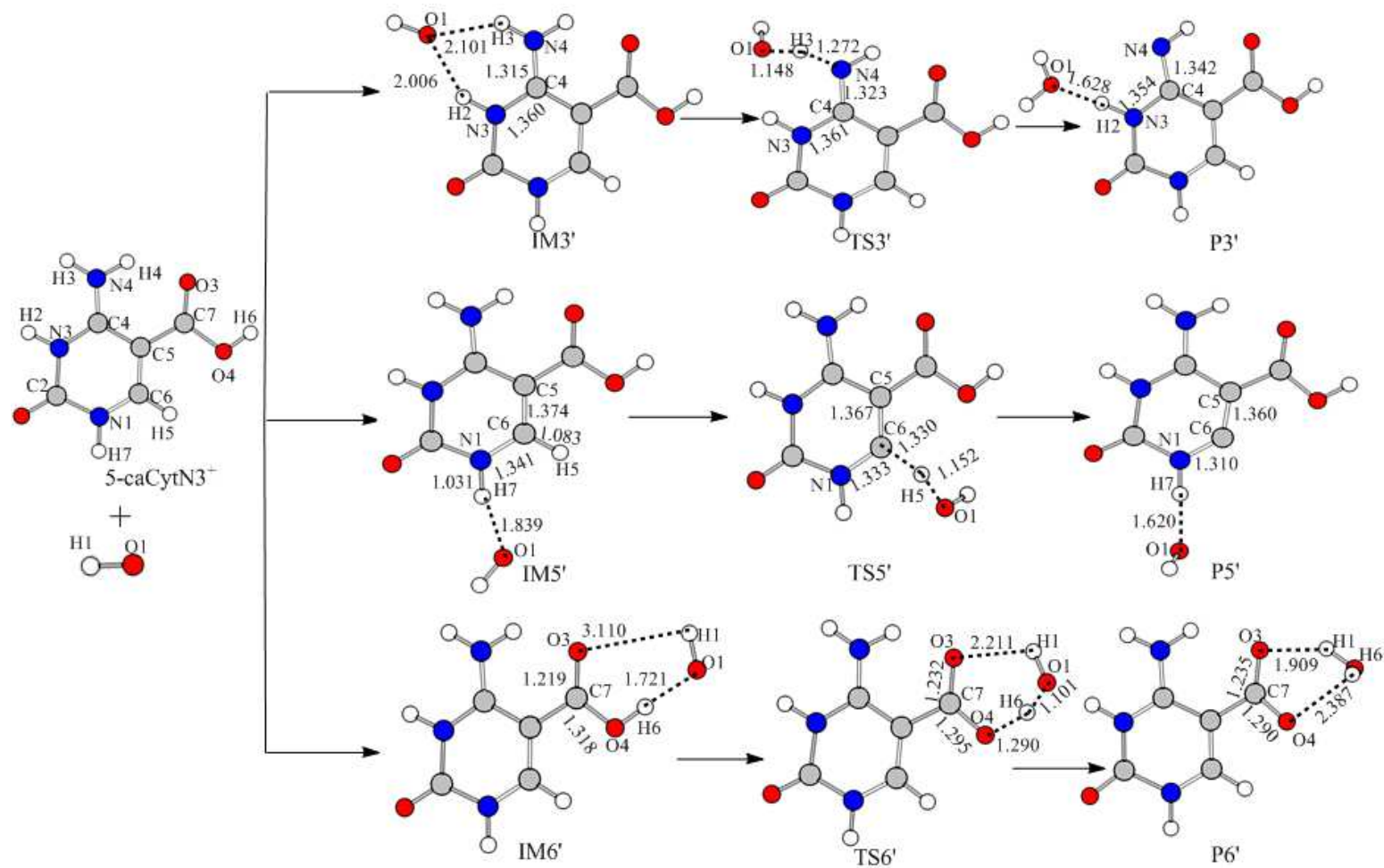


Fig. 9

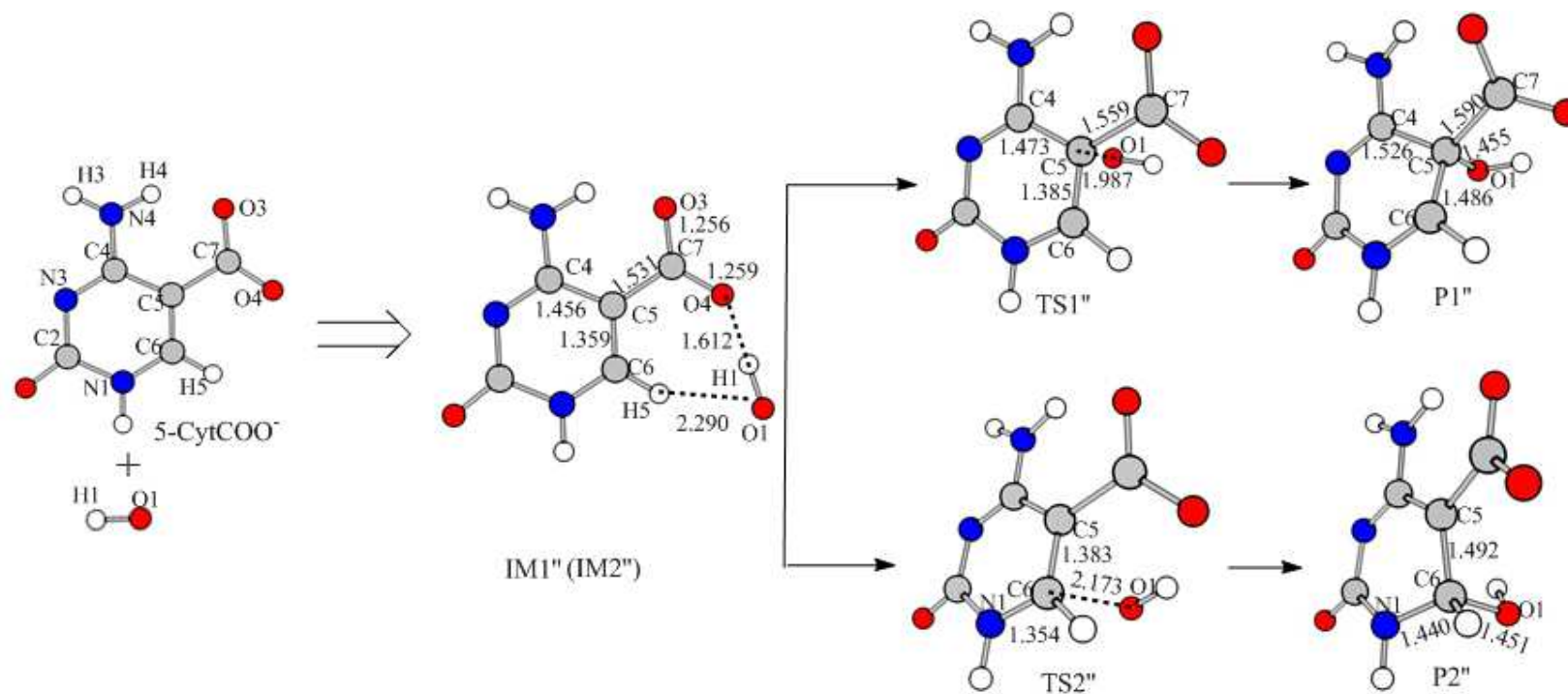


Fig. 10

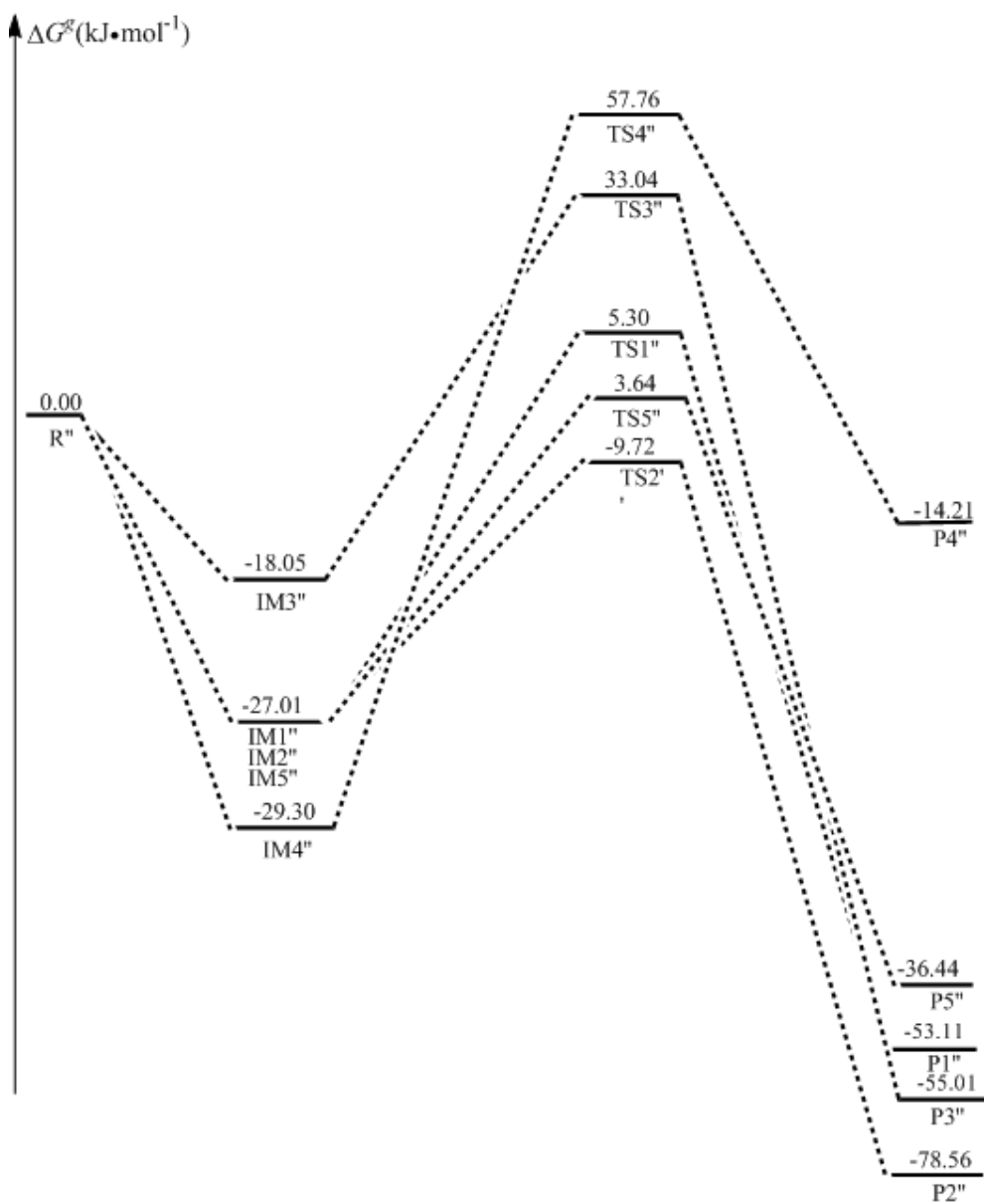


Fig.11

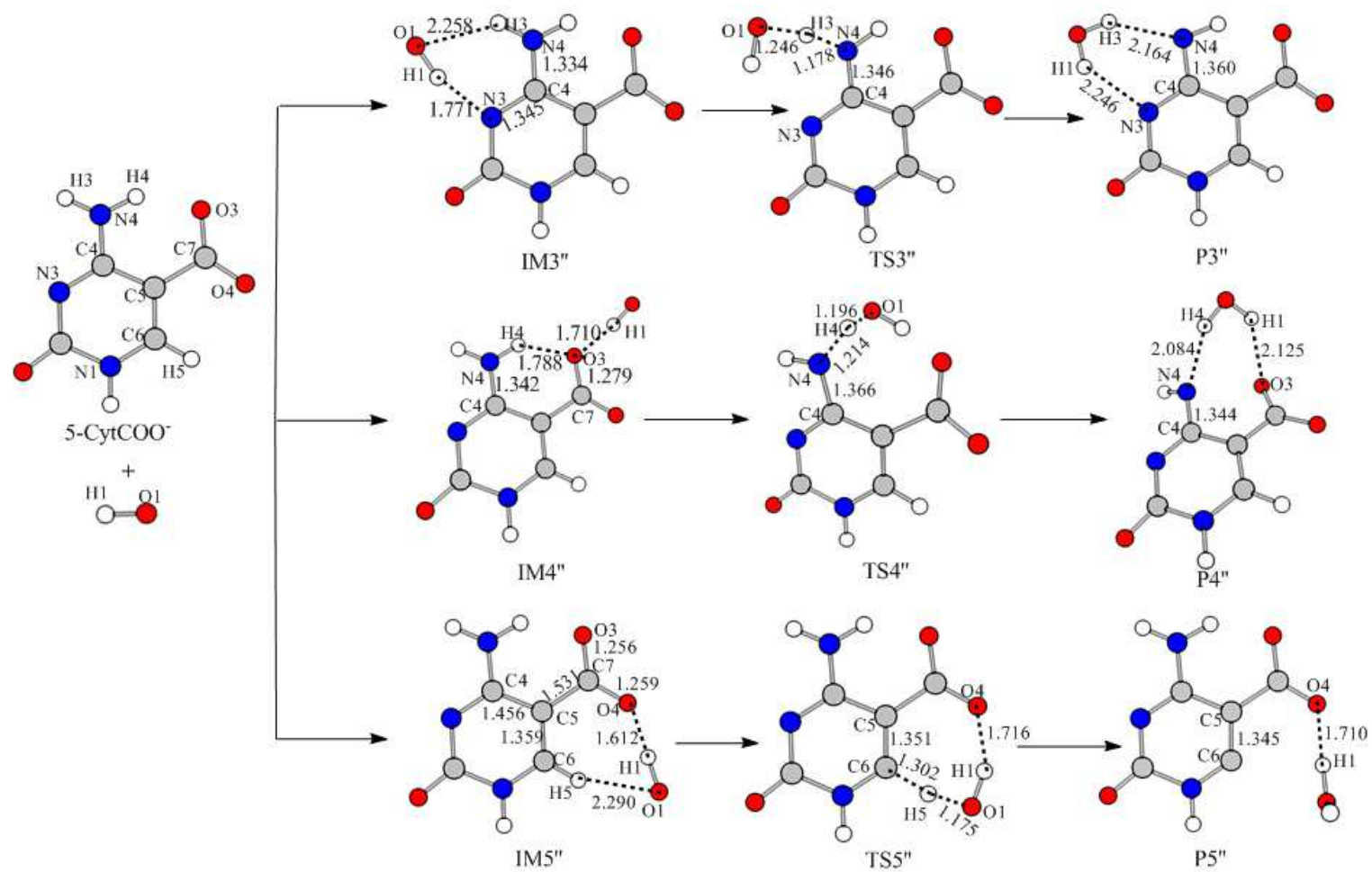
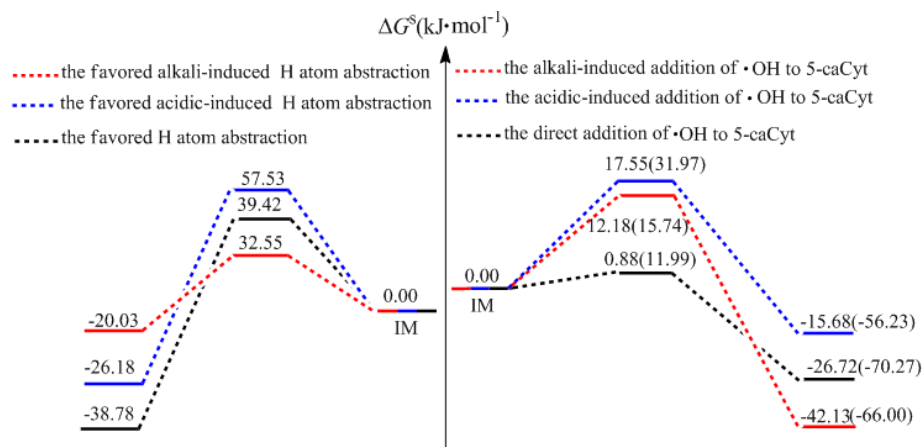


Fig. 12

Graphical Abstract

Effects of Acid-alkaline Environment on the Reactivity of the 5-Carboxycytosine with Hydroxyl Radical

Lingxia Jin Caibin Zhao Tianlei Zhang Zhiyin Wang Suotian Min Wenliang Wang Yawen Wei



The addition of •OH to C5=C6 double bond and abstraction of H5 from 5-caCyt is more favourable in neutral, acid and alkaline conditions. The ΔG^{\ddagger} of C5 channel is a little higher than C6 route, which agrees with the tendencies observed experimentally. Moreover, the H5 abstraction in alkaline media might be competitive with the addition reactions, having a ΔG^{\ddagger} value of 32.55 $\text{kJ}\cdot\text{mol}^{-1}$, which is only 17-20 $\text{kJ}\cdot\text{mol}^{-1}$ more energetic than the results for the addition reactions.